

Paper 67-3 has been designated as a Distinguished Student Paper at Display Week 2025. The full-length version of this paper appears in a Special Section of the *Journal of the Society for Information Display (JSID)* devoted to Display Week 2025 Distinguished Papers. This Special Section will be freely accessible until December 31, 2025 via:

<https://sid.onlinelibrary.wiley.com/doi/full/10.1002/jsid.2055>

Authors that wish to refer to this work are advised to cite the full-length version by referring to its DOI:

<https://doi.org/10.1002/jsid.2055>

Improvement of Photostability and Clarification of Suitable Substituent Space of Zwitterionic Ligands for CsPbBr₃ Perovskite Nanocrystals

Takuro Iizuka (Master student)¹, Yusaku Morikawa¹, Taisei Kimura¹, Motofumi Kashiwagi², Satoshi Asakura³, Akito Masuhara^{1,4}

¹Grad. Sch. of Sci. and Eng., Yamagata Univ., 4-3-16 Jonan, Yonezawa, Yamagata 992-8510, Japan

²ZEON Corp., 1-6-2 Marunouchi, Chiyoda-ku, Tokyo 100-8246, Japan

³ISE CHEMICALS Corp., 1-3-1 Kyobashi, Chuo-ku, Tokyo 104-0031, Japan

⁴FROM, Yamagata Univ., 4-3-16 Jonan, Yonezawa, Yamagata 992-8510, Japan

Abstract

Lead halide perovskite nanocrystals (PeNCs) have not been clarified regarding the factors that affect the improvement in photostability by zwitterionic ligands.

Therefore, we focused on the substituent space in the zwitterionic ligands and clarified the mechanism for improving the photostability of PeNCs with zwitterionic ligands. We clarified that the key factor in the improvement of photostability by zwitterionic ligands is the ligand ratio on the PeNCs surface caused by the substituent space. SB3, a synthesized ligand with the number of carbons between substituents of 3, occupied 87.4% of the surface, and this ratio was significantly higher than the ratio of ligands with other substituent spaces. This critically affected the photostability, and PeNCs with SB3 successfully maintained the PLQY after 30 h of photoirradiation ($\lambda_{\text{exc}} = 450 \text{ nm}$; Irradiation Intensity = 30 mW/cm²).

Keywords

Perovskite nanocrystal, LCD, Zwitterionic ligand, Sulfobetaine, Photostability

1. Introduction

Lead Halide Perovskite nanocrystals (CsPbX₃, X = Cl, Br, and I) are promising next-generation photoconversion materials for various optoelectronic devices, such as solar cells [1], enhancement conversion films [2], LED (light-emitting diodes) [3], lasers, and X-ray detectors [4] (Figure 1). Their outstanding and excellent optical properties include high luminescence quantum yield (PLQY), narrow full width at half maximum (FWHM), and easily tunable photoluminescence due to the crystal size or mixing halide [5]. Because of these excellent optical properties, PeNCs were used as optical materials to compare pristine CdSe and InP QDs. Furthermore, PeNCs can satisfy the latest television standard BT. 2020 and have the potential to be ultimate displays [6] [7]. However, PeNCs have issues that strongly support their stability. [6].

The PeNCs were protected by capping their surfaces with ligands.

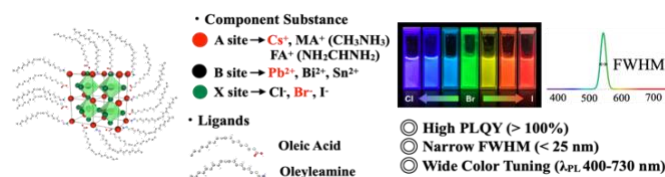


Figure 1. Crystal structure of cesium lead trihalide perovskite. Appearance and features of the perovskite nanocrystals.

Typically, oleic acid and oleylamine are used as ligands. It has been reported that these ligands repeatedly absorb and desorb on the surface of PeNCs owing to the acid-base equilibrium [8] [9]. Ligands are electrically absorbed on the PeNC through the

exchange of protons between the carboxylic acid and amine groups. In other words, the ligands dynamically capped the PeNC surface by continuously transitioning between ionic and non-ionic substituents through proton exchange.

However, the PLQY of the PeNCs dramatically decreased under strong photoirradiation, assuming a backlight display. In general, the photodegradation process is as follows. ①The surface ligands momentarily desorb from the PeNC surface. ②The surface leads are exposed to the external environment. ③The exposed leads are oxidized or reduced and converted from Pb²⁺ to Pb⁴⁺ or Pb⁰ due to oxygen or photo energy [10] [11]. ④The desorbed ligands are prevented from reabsorbing onto the surface because the charge state of the exposed lead atoms has changed. These processes result in the formation of numerous surface defects on the PeNCs and aggregation of the PeNCs. Furthermore, the trap levels in the energy band gap were formed due to these surface defects, hindering effective carrier recombination in the PeNCs [12].

Therefore, the degradation mechanism must be suppressed, which poses a significant challenge to the application of PeNCs in displays. Zwitterionic ligands have been proposed to solve this problem. [6] [13] Ordinarily, ligands were composed of a head group that absorbs onto PeNCs and a tail group that is composed of a long alkyl chain that contributes to the dispersibility of the PeNCs. In contrast, zwitterionic ligands feature a head group composed of a cation, anion, and an alkyl chain that bridges them. The number of carbons in the alkyl chain controls the distance between the substituents. For example, sulfobetaine-type ligands, which consist of a quaternary ammonium group and sulfonic acid, and phosphocholine-type ligands, which consist of quaternary ammonium and phosphonic acid, are widely used as zwitterionic ligands.

The head groups in zwitterionic ligands provide excellent passivation of PeNCs owing to their non-dynamic binding to the PeNC surface without acid-base equilibrium [6] [13]. Additionally, it has been reported that zwitterionic head groups selectively influence the crystal morphology of the PeNCs. This phenomenon is suggested to result from differences in the binding energies of the ligands, which depend on the distance between substituents [14]. Obviously, zwitterionic head groups are known to have a positive effect on the photostability of PeNCs. [15].

However, the origin of the positive effects of the zwitterionic head group on the photostability remains unknown. Photostability of PeNCs is the most important for display applications, and a comprehensive understanding of the effect will play a significant role in advancing research on PeNCs stabilization. In addition, the relationship between the substituent space in zwitterionic ligands and the photostability of PeNCs has not yet been clarified, even though space plays an important role in the ligand behavior.

In this study, we identified a key factor that improves the photostability of PeNCs when zwitterionic ligands are used, specifically focusing on the impact of the substituent space within the ligands. We synthesized sulfobetaine-type ligands with substituent spacings corresponding to carbon chain lengths of 2, 3, and 4, labeled SB2, SB3, and SB4, respectively (Figure 2). Surprisingly, we found that differences in substituent spacing significantly changed the ligand ratios on the PeNC surface, which was directly correlated with photostability. We achieved a PLQY of 100% for PeNCs with SB3 after 30 h under continuous photoirradiation.

2. Experimental

Synthesize of controlled substituent space sulfobetaine - type zwitterionic ligands: Each controlled zwitterionic ligands were synthesized according to previous studies[16] [17].

SB2: *N, N*-Dimethyl octadecylamine and sodium 2- chloroethane sulfonate monohydrate were dissolved in *N, N*-dimethylformamide (DMF), and the solution was heated for 4 days at 160°C. The crude product was washed thrice with diethyl ether. Finally, the washed products were purified by recrystallization from DMF three times.

SB3, SB4: *N, N*-dimethyl octadecylamine, and 1,3-propanesultone or 1,4-butanedisultone were dissolved in acetonitrile, and the solution was heated to proceed reaction for 1 day at 75°C. Subsequently, the crude product was purified using the same process as that used for SB2.

Preparation of CsPbBr₃ PeNCs with each candidate ligand

CsPbBr₃ PeNCs were prepared as previously described, with modifications at room temperature (Figure 2) [18]. A Pb precursor solution was prepared with lead bromide (PbBr₂) and tri-*n*-octylphosphine oxide (TOPO) in toluene. A Cs precursor solution was prepared using cesium carbonate (CsCO₃) and oleic acid (OA) in toluene. A ligand exchange solution was prepared with each candidate ligand in propylene carbonate and toluene. For comparison, octadecyltrimethylammonium bromide was dissolved in the solvent as a reference sample.

The Cs precursor solution was mixed with the Pb precursor under vigorous stirring to prepare the PeNCs. Subsequently, the ligand exchange solution was added to the obtained PeNCs dispersion. For purification, the PeNCs were centrifuged several times, and the PeNCs were collected and purified. The PeNCs dispersion was measured in the PL spectra, and the optical properties were evaluated. PeNCs were coordinated with each candidate ligand and labeled as PeNCs@Ref., PeNCs@SB2, PeNCs@SB3, and PeNCs@SB4.

Quantification of ligand ratio on PeNC surface

The ratio of the candidate ligands on the PeNCs was quantified by ¹H NMR using the following process. First, the concentration of the PeNCs was adjusted identically for each sample. The dispersant was then completely removed by the evaporators. The dried PeNCs were then dissolved in DMSO-*d*₆ with maleic acid as a reference to obtain ¹H NMR spectra. From the spectra, each ligand ratio was calculated to compare the spectra of the peak derived from its ligands with the reference maleic acid [19].

Photostability evaluation of PeNCs dispersion:

The concentration of PeNCs in each ligand was determined based on absorbance. Finally, photoirradiation ($\lambda_{ex} = 450 \text{ nm}$, 30 mW/cm²) was carried out under atmospheric conditions to evaluate the optical properties of the CsPbBr₃ PeNCs dispersion from the PL spectra.

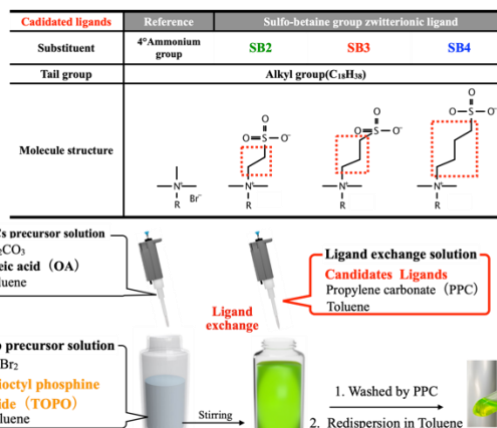


Figure 2. Molecular structures of candidate ligands and schematic illustration of the synthesis process of PeNCs with candidate ligands.

3. Result and Discussion

Optical properties of the PeNCs with zwitterionic ligands:

The ¹H NMR spectra of each controlled zwitterionic ligand are shown in Figure 3a. These structures were confirmed, and distinct peaks originating from controlled substituent space were observed [16] [17].

The SEM-EDX mapping images of the PeNCs with each zwitterionic ligand are shown in Figure 3b. Sulfur, a characteristic element of ligands, was detected in the PeNCs. Therefore, it was demonstrated that these ligands coordinated with PeNCs.

The PL spectra of the PeNCs with candidate ligands and their optical properties are shown in Table 1 and Figure 3c. All PeNCs dispersions with the candidate ligands exhibited a single emission peak at 517 nm. The emission peak did not depend on the ligands. In addition, all PeNCs with candidate ligand dispersions exhibited high PLQY of up to 80%.

We successfully synthesized PeNCs with excellent optical properties. In particular, PeNCs @SB3 and SB4 increased the PLQY by up to 100% owing to well-passivated surface defects. This indicates that the zwitterionic ligands, particularly SB3 and SB4, can be easily absorbed on the PeNC surface and remove surface defects to strongly suppress non-radiative recombination.

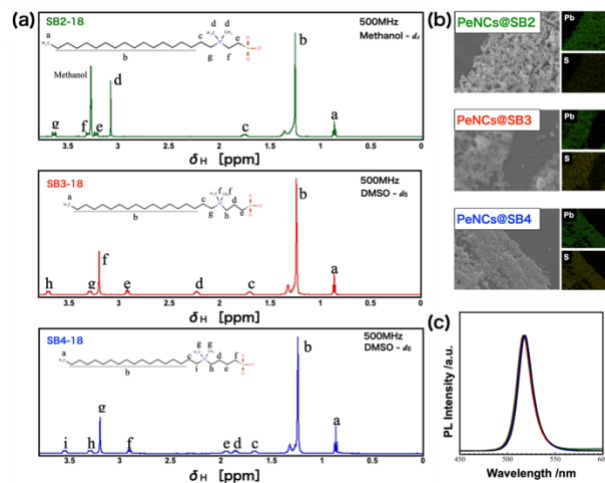


Figure 3. ¹H NMR spectra of synthesized zwitterionic ligands (a). and SEM – EDX mapping images of lead, and Sulfur (b). PL spectra of all PeNC dispersions (c).

Table 1. Optical properties of PeNCs with candidate ligand dispersions (The excitation wavelength : 370 nm)

Sample	λ_{PL} /nm	FWHM /nm	PLQY /%
PeNCs@Ref.	517	18	81
PeNCs@SB2	517	20	86
PeNCs@SB3	517	18	100
PeNCs@SB4	517	17	100

Quantitative evaluation of the ligand ratio on the PeNC surface

The ratio of candidate ligands on the PeNCs was quantified using ^1H NMR spectroscopy. The NMR spectra of the PeNCs with candidate ligands are shown in Figure 4. In these spectra, the reference maleic acid showed a peak at 6.20 ppm, while oleic acid and TOPO, which were used in the synthesis of PeNCs, exhibited independent peaks at 5.28 and 1.52 ppm, respectively. Furthermore, in Ref., SB2, SB3, and SB4, distinct peaks originating from these ligands are observed at 2.98, 2.96, 2.96, and 2.96 ppm, respectively. The ratios of candidate ligands were calculated from the peak areas, as shown in Table 2.

As a result, SB2 occupied only 16.4%, whereas TOPO occupied 71.1% of the surface in the case of PeNCs@SB2. SB4 occupied 59.8%, but TOPO occupied 33.8% of the surface in the case of PeNCs @ SB4. In contrast, SB3 occupied 87.4%, whereas TOPO occupied 10.9% in the case of PeNCs @ SB3. These results indicate that the difference in the substituent space in the zwitterionic ligands is an important factor in the ease of bonding on the PeNCs.

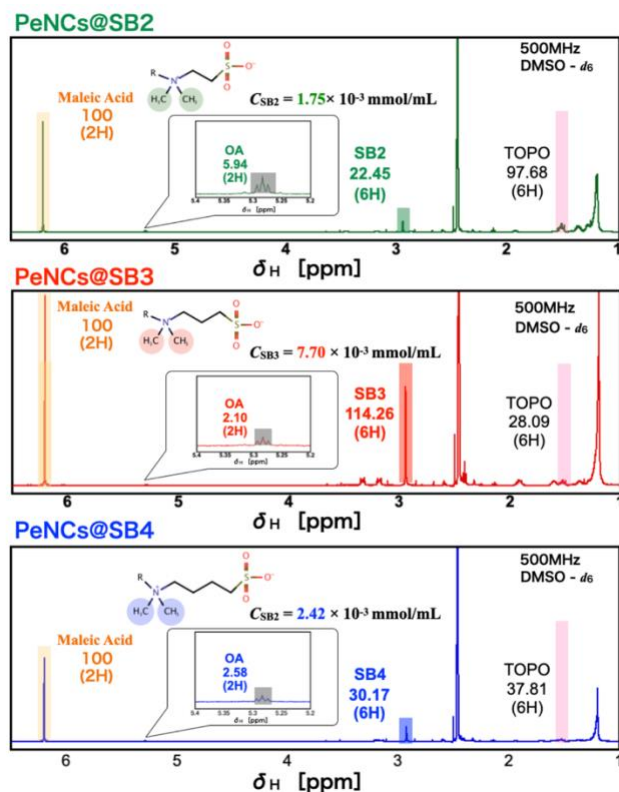


Figure 4. ^1H NMR spectra of the surface ligands on PeNCs.

Table 2. Candidate ligand ratios for all ligands on the PeNCs surface.

sample	Ligand ratio /%
	Candidate Ligand
PeNCs@Ref.	57.7
PeNCs@SB2	26.4
PeNCs@SB3	87.4
PeNCs@SB4	59.8

Photostability evaluation of the PeNCs with candidate ligand dispersions :

Photostability evaluation was performed under photoirradiation ($\lambda_{ex.} = 450$ nm, Irradiation intensity = 30 mW/cm²) for the PeNCs with candidate ligand dispersions (Figure 5a).

In the result, PeNCs @ SB3 achieved to maintain a PLQY of 100% after 30 h. PeNCs @ SB3 showed clearly excellent dispersibility, and the λ_{PL} and FWHM values were the same before irradiation.

This indicates that the surface ligands were not desorbed from the PeNCs by photo energy because of the high ratio of SB3 on the surface and strong bonding as a chelation with PeNCs [20]. The aggregation of PeNCs was prevented by maintaining the ligand absorption on the surface. However, except for PeNCs @ SB3, the PLQY decreased with increasing irradiation time. PeNCs with surface defects were exposed by desorption of the surface ligands. Furthermore, these PeNCs turned into bulk crystals because they aggregated with the other PeNCs (Figure 5b). The PeNCs dispersion of the emission wavelength was red-shifted, and the

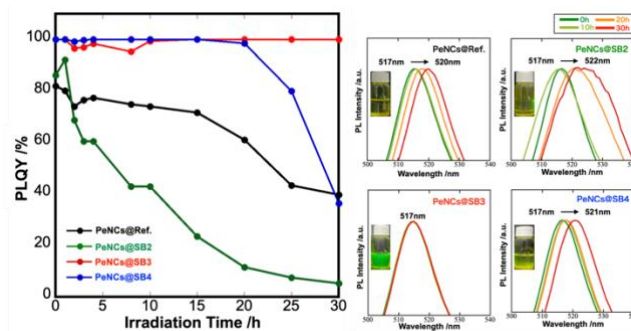


Figure 5. The results of photostability evaluation of PeNCs dispersions with candidate ligands (a). The change in emission wavelength and its appearance under photo irradiation (b).

FWHM was broader than that before photoirradiation.

4. Summary

In summary, we clarified the relationship between the substituent space in zwitterionic ligands and the stability of PeNCs.

We also demonstrated how the substituent distance in the sulfobetaine-type zwitterionic ligands influences the ligand ratio on the PeNC surface. Specifically, SB2 occupied 16.4%, SB3 for 87.4%, and SB4 for 59.8% of the total ligands on the surface. This evaluation clarified for the first time that the difference in substituent distance in zwitterionic ligands dramatically affected the ligand ratio on the PeNC surface.

Furthermore, in the photostability evaluation, we observed that the difference in the ligand ratio on the surface strongly correlates with long-term dispersibility. PeNCs @ SB3 achieved a perfect PLQY of 100% after 30h of photoirradiation.

We identified the relationship between the improvement in photostability and the dependency of the surface ligand ratio. Thus,

this study provides a new perspective on the photostability of the PeNCs.

5. Acknowledgments

The authors would like to thank “A-STEP (Adaptable and Seamless Technology transfer Program through Target-driven R&D) from JST, Grant Number JPMJTR223B”, and “Dynamic Alliance for Open Innovation Bridging Human, Environment and Materials” in Network Joint Research Center for Materials and Devices, Grant Number 20244005”, Master 21 scholarship from Yoshida Scholarship Foundation.

6. References

1. Michael ML, Joël T, Tsutomu M, Takurou NM, Henry JS. Efficient Hybrid Solar Cells Based on Meso-Superstructured Organometal Halide Perovskites. *Science*. 2012;338(6107).
2. Hu, H., Levchuk, I., Kalkowski, F., Elia, J., Osvet, A., & Brabec, C. J. (2023). Engineering Stable Perovskite Film for High Color Purity Display Application. *ACS Energy Letters*, 8(10), 4380-4385.
3. Pan, Q., Hu, J., Fu, J., Lin, Y., Zou, C., Di, D., Wang, Y., Zhang, Q., & Cao, M. (2022). Ultrahigh Stability of Perovskite Nanocrystals by Using Semiconducting Molecular Species for Displays. *ACS Nano*, 16(8), 12253-12261.
4. Chen, Q., Wu, J., Ou, X., Huang, B., Almutlaq, J., Zhumekenov, A. A., Guan, X., Han, S., Liang, L., Yi, Z., Li, J., Xie, X., Wang, Y., Li, Y., Fan, D., Teh, D. B. L., All, A. H., Mohammed, O. F., Bakr, O. M.,...Liu, X. (2018). All-inorganic perovskite nanocrystal scintillators. *Nature*, 561(7721), 88-93.
5. Goto, M., Oshita, N., Yoshida, K., Iizuka, T., Morikawa, Y., Shimizu, H., Kobayashi, R., Chiba, T., Asakura, S., & Masuhara, A. (2024). Blue-emitting perovskite nanocrystals with enhanced optical properties through using NaBH₄. *Applied Physics Express*, 17(7).
6. Mir, W. J., Alamoudi, A., Yin, J., Yorov, K. E., Maity, P., Naphade, R., Shao, B., Wang, J., Lintangpradipto, M. N., Nematulloev, S., Emwas, A. H., Genovese, A., Mohammed, O. F., & Bakr, O. M. (2022). Lecithin Capping Ligands Enable Ultrastable Perovskite-Phase CsPbI₃ Quantum Dots for Rec. 2020 Bright-Red Light-Emitting Diodes. *J Am Chem Soc*, 144(29), 13302-13310.
7. Zhang, Q., Sun, X., Zheng, W., Wan, Q., Liu, M., Liao, X., Hagio, T., Ichino, R., Kong, L., Wang, H., & Li, L. (2021). Band Gap Engineering toward Wavelength Tunable CsPbBr₃ Nanocrystals for Achieving Rec. 2020 Displays. *Chemistry of Materials*, 33(10), 3575-3584.
8. De Roo, J., Ibáñez, M., Geiregat, P., Nedelcu, G., Walravens, W., Maes, J., Martins, J. C., Van Driessche, I., Kovalenko, M. V., & Hens, Z. (2016). Highly Dynamic Ligand Binding and Light Absorption Coefficient of Cesium Lead Bromide Perovskite Nanocrystals. *ACS Nano*, 10(2), 2071-2081.
9. De Roo, J., Coucke, S., Rijckaert, H., De Keukeleere, K., Sinnaeve, D., Hens, Z., Martins, J. C., & Van Driessche, I. (2016). Amino Acid-Based Stabilization of Oxide Nanocrystals in Polar Media: From Insight in Ligand Exchange to Solution (1)H NMR Probing of Short-Chained Adsorbates. *Langmuir*, 32(8), 1962-1970.
10. Dang, Z., Shamsi, J., Palazon, F., Imran, M., Akkerman, Q. A., Park, S., Bertoni, G., Prato, M., Brescia, R., & Manna, L. (2017). In Situ Transmission Electron Microscopy Study of Electron Beam-Induced Transformations in Colloidal Cesium Lead Halide Perovskite Nanocrystals. *ACS Nano*, 11(2), 2124-2132.
11. An, R., Zhang, F., Zou, X., Tang, Y., Liang, M., Oshchapovskyy, I., Liu, Y., Honarfar, A., Zhong, Y., Li, C., Geng, H., Chen, J., Canton, S. E., Pullerits, T., & Zheng, K. (2018). Photostability and Photodegradation Processes in Colloidal CsPbI₃ Perovskite Quantum Dots. *ACS Appl Mater Interfaces*, 10(45), 39222-39227.
12. Sun, W., Yun, R., Liu, Y., Zhang, X., Yuan, M., Zhang, L., & Li, X. (2023). Ligands in Lead Halide Perovskite Nanocrystals: From Synthesis to Optoelectronic Applications. *Small*, 19(11), e2205950.
13. Zu, Y., Xi, J., Li, L., Dai, J., Wang, S., Yun, F., Jiao, B., Dong, H., Hou, X., & Wu, Z. (2020). High-Brightness and Color-Tunable FAPbBr₃ Perovskite Nanocrystals 2.0 Enable Ultrapure Green Luminescence for Achieving Recommendation 2020 Displays. *ACS Applied Materials & Interfaces*, 12(2), 2835-2841.
14. Amador-Sanchez, Y. A., Vargas, B., Romero-Ibarra, J. E., Mendoza-Cruz, R., Ramos, E., & Solis-Ibarra, D. (2024). Surfactant-tail control of CsPbBr₃ nanocrystal morphology. *Nanoscale Horiz*, 9(3), 472-478.
15. Liu, Y., Xie, Q., Ying, Y., Gao, Z., Shao, X., Xia, W., Zhou, M., Pei, W., Tang, X., & Tu, Y. (2024). Ostwald ripening inhibition by a bipolar ligand achieves long-term-reaction and scalable synthesis of ultra-stable CsPbX₃ perovskite quantum dots towards LEDs. *Chemical Engineering Journal*, 498.
16. Wang, M.-L., & Hsieh, Y.-M. (2007). Kinetic Study of the Synthesis of Dichlorocyclopropane by Trialkylammonium Propansulfates as New Phase-Transfer Catalysts. *Chemical Engineering Communications*, 194(4), 477-494.
17. Ward, R. S., Davies, J., Hodges, G., & Roberts, D. W. (2002). Synthesis of quaternary alkylammonium sulfobetaines. *Synthesis-Stuttgart*(16), 2431-2439.
18. Akkerman, Q. A., Nguyen, T. P. T., Boehme, S. C., Montanarella, F., Dirin, D. N., Wechsler, P., Beiglbock, F., Raino, G., Erni, R., Katan, C., Even, J., & Kovalenko, M. V. (2022). Controlling the nucleation and growth kinetics of lead halide perovskite quantum dots. *Science*, 377(6613), 1406-1412.
19. Kimura, T., Yamakado, R., Oshita, N., Asakura, S., & M Asuhara, A. (2022). Thickness control of perovskite nanocrystals based on the molecular structure of surface ligands. *Applied Physics Express*, 15(10), 105502.
20. Krieg, F., Ochsenbein, S. T., Yakunin, S., Ten Brinck, S., Aellen, P., Stuess, A., Clerc, B., Guggisberg, D., Nazarenko, O., & Shynkarenko, Y. (2018). Colloidal CsPbX₃ (X= Cl, Br, I) nanocrystals 2.0: Zwitterionic capping ligands for improved durability and stability. *ACS Energy Letters*, 3(3), 641-646.